J. Fluid Mech. (2010), *vol.* 655, *pp.* 527–539.
doi:10.1017/S0022112010001734

On the growth of the mixing zone in miscible viscous fingering

R. J. S. BOOTH†

Mathematical Institute, Oxford University, 24–29 Saint Giles, Oxford OX1 3LB, UK

(Received 11 August 2009; revised 7 April 2010; accepted 8 April 2010;

We investigate the growth of a mixing zone in the displacement of oil by a solvent. Such a zone usually takes the form of long thin fingers of solvent which protrude into the oil. However, despite the existence of reasonably good empirical models for the evolution of mixing zones, there is limited theoretical understanding of the observed growth. Of particular interest is the rate at which the leading edge of the mixing zone grows. In this paper we establish the structure of the mixing zone, and reveal a critical mechanism that plays a role in the growth of the leading edge of the mixing zone. It turns out that there is a close link between the growth rate of the mixing zone and a shape selection problem for Saffman–Taylor fingers.

Key words: convection in porous media, fingering instability, mixing and dispersion

1. Introduction

The existence of a viscous fingering instability when a less viscous fluid displaces a more viscous fluid, either in a porous medium or a Hele-Shaw cell, has been well documented (Saffman & Taylor 1958; Homsy 1987). One of the most important properties of the viscous fingering instability is that the smallest wavelength disturbances generally grow fastest, although mechanisms such as diffusion or a diffuse initial condition typically lead to the existence of a cutoff or least stable wavelength (see Hickernell & Yortsos 1986; Tan & Homsy 1986; Riaz, Pankiewitz & Meiburg 2004), leading to the expectation that small-wavelength fingers will form. This type of instability is suggestive of an ill-posed problem and indeed the simplest model of the displacement of two fluids with contrasting viscosity, the Muskat problem, has been shown in Siegel, Caflisch & Howison (2004) to develop singularities in the curvature of the interface between the two fluids. In enhanced oil recovery, either a hydrocarbon solvent or supercritical carbon dioxide may be used to displace oil from an oil reservoir. This leads to a miscible displacement between the two fluids with molecular diffusion between the two fluids and a smoothly varying viscosity, which may be modelled by

$$\nabla \cdot \boldsymbol{u} = 0, \tag{1.1}$$

$$\boldsymbol{u} = -\frac{k}{\mu(c)}\nabla p, \tag{1.2}$$

$$\phi\frac{\partial c}{\partial t} + \nabla \cdot (\boldsymbol{u}c) = D\nabla^2 c, \tag{1.3}$$

---

† Email address for correspondence: rjsbooth@gmail.com

where $\boldsymbol{u}$ is the total flux of fluid per unit area, k is the permeability of the medium, c is the volume fraction of solvent, p is the pressure in the fluid; also, $\mu(c)$ is the viscosity of a homogeneous mixture of oil and solvent with a volume fraction c of solvent which is taken (see Koval 1963) as

$$\mu(c) = \left(\mu_s^{-1/4}c + \mu_o^{-1/4}(1-c)\right)^{-4}, \tag{1.4}$$

where μ_s and μ_o are the viscosities of pure solvent and pure oil, respectively. This model is well posed (see Mikelić 1993).

In (1.3) we treat diffusion as isotropic and constant with diffusion coefficient D; however, in the real problem such a model for diffusion will not necessarily hold true due to the effect of hydrodynamic dispersion. The above model also neglects the effect of gravity which is permissible when either the densities of the two fluids approximately match, the applied pressure gradients are large, or when the flow is in a thin horizontal layer. We believe that the essential behaviour of the physical problem can often be captured by this more simple model, but we shall later make note of instances where different models of diffusion may lead one to different conclusions.

The model (1.1)–(1.3) can be non-dimensionalized with lengths scaled by the size of the reservoir L, and the time scaled by $\phi L/U$, where U is representative of the flux of fluid in the reservoir. On non-dimensionalization we find that the behaviour of the model depends on two important non-dimensional parameters: the Péclet number $Pe = UL/D$, being the ratio between the time scale for diffusion and the time scale for convection, and the mobility ratio $M = \mu_o/\mu_s$. In enhanced oil recovery processes the Péclet number will be large and the mobility ratio will be greater than 1.

There have been numerous numerical simulations of (1.1)–(1.3) (Peaceman & Rachford 1962; Tan & Homsy 1988; Zimmerman & Homsy 1991, 1992; Christie, Muggeridge & Barley 1993; Rogerson & Meiburg 1993; Tchelepi *et al.* 1993; Tchelepi & Orr 1994; Chen & Meiburg 2000; Ruith & Meiburg 2000; Yang, Yortsos & Salin 2002; Riaz & Meiburg 2003) which have all shown that viscous fingers will still form provided that the Péclet number is sufficiently large. When the Péclet number is very large it has been observed that the width of the fingers is small, and accurate numerical solution is costly. Although the detailed fingering pattern may be difficult to reproduce, the numerical simulations of Zimmerman & Homsy (1992) and Yang *et al.* (2002) have suggested that the mean concentration of solvent, averaged across the fingers, may be much simpler to describe. This is especially true when the geometry of the problem is quite simple such as a linear flood, where the applied pressure gradient is solely in the x direction. Empirical models are available which attempt to model the mean transport of the solvent through the reservoir, the simplest of which is due to Koval (1963) and is given by

$$\frac{\partial \bar{c}}{\partial t} + U\frac{\partial}{\partial x}\left(\frac{M_e\bar{c}}{1+(M_e-1)\bar{c}}\right) = 0, \tag{1.5}$$

where $\bar{c}$ is the volume concentration of solvent averaged across the fingers, U is the total flux of fluid and M_e is an 'effective' mobility ratio, defined by

$$M_e = \left(0.22M^{1/4} + (1-0.22)\right)^4, \tag{1.6}$$

where the value 0.22 has been chosen to fit with the empirical recovery data of Blackwell, Rayne & Terry (1959).

The Koval model is also supported by numerical simulations of (1.1)–(1.3) in Yang *et al.* (2002) and Booth (2008), when the Péclet number is large. The Koval model should be thought of as an *ad-hoc* fit to the available data from experiments and numerical simulations and it has no rigorous derivation. Efforts have been made in Todd & Longstaff (1972), Fayers (1988) and Fayers, Blunt & Christie (1992) to produce an empirical model that both fits the data and gives a reasonably accurate description of the internal structure of the viscous fingering. These models are capable of matching not only the growth rate of the fingering region but also the pressure drop through the fingering region, and allow for fully three-dimensional simulations with the possible inclusion of gravity segregation. Ultimately all of these models rely on some *ad-hoc* matching with data from physical experiments (see Blackwell *et al.* 1959; Tchelepi *et al.* 1993) and numerical simulations. In the case of the model by Todd and Longstaff (Todd & Longstaff 1972), as with that of Koval (Koval 1963), there is only a single matching parameter, whereas the Fayers model (Fayers 1988) introduces a more sophisticated 'fingering function'. The model by Todd and Longstaff is widely used for simulating miscible flow in real-world reservoir engineering applications.

One of the most important features of the Koval model is that, as a hyperbolic equation, it predicts that there is a finite speed at which the mixing zone can encroach into the oil. This speed is equal to UM_e, and may be interpreted as the speed at which the leading finger tips must travel. As noted in Yortsos & Salin (2006), this observed speed of the finger tips is much lower than a naïve analysis would suggest. If a region of pure solvent and a region of pure oil were to be acted on by the same pressure gradient then by (1.2) the velocity of the solvent region would be M times faster than the velocity of the oil region. One might therefore expect that it is possible for a small volume of solvent in the leading finger tips to travel with a speed equal to UM, which is much faster than the observed speed. An explanation as to why the mixing zone spreads at the rate predicted by the Koval model (Koval 1963) is required to understand the averaged behaviour of miscible viscous fingers.

As an aside we make note of the important relationship between miscible viscous fingering and miscible density fingering as described by Wooding (1969). When the viscosity ratio between the two fluids is close to 1, it is possible to show that, with a rescaling of diffusion, the two problems are equivalent Manickam & Homsy (1995). Furthermore, one finds that the growth rate of the mixing zone as suggested by Koval for viscous fingering agrees with the observations of Wooding (1969) of miscible density fingering in Hele-Shaw cells. This agreement provides further support for the validity of the Koval model over a wide range of values of M.

In this paper we establish an idealized model for the structure of fingering in the mixing zone, and thereby deduce a possible explanation for the observed growth rate of the mixing zone.

2. Homogenized model of fingering

In order to compare our theory with the Koval model, and much of the physical and numerical experiments available, we consider a simple two-dimensional linear flood with an applied pressure gradient in the x direction, the strength of the pressure gradient chosen to ensure that there is a constant flux of fluid through the reservoir. We can gain a basic insight into the formation of fingers by considering the linear stability of (1.1)–(1.3).

In contrast to the linear stability analysis of the Muskat problem there is a maximum rate of growth of disturbances and both a least stable wavelength and cutoff wavelength so that all disturbances of wavelength less than the cutoff wavelength are stable (Tan & Homsy 1986). As the Péclet number increases the least stable wavelength and the cutoff wavelength both decrease, suggesting that the width of fingers will decrease as the Péclet number increases. Both linear stability analysis and numerical simulations (see Booth 2008) suggest that for $Pe \gg 1$ the typical width of the fingers is proportional to $Pe^{-1/2}$. It is also possible to predict the $Pe^{-1/2}$ scaling by noting that it is the only scaling which ensures that neither diffusion nor convection are negligible in (1.3) as $Pe \to \infty$. The width of fingers depends on Pe which in turn depends on the length of the domain. This fact seems peculiar, however it should be understood that it is not directly the length L of the domain, but the induced time scale L/U, that controls the width of fingers.

We therefore propose that the mixing zone is constructed of many long thin fingers with the aspect ratio of the fingers proportional to $Pe^{-1/2}$, each aligned approximately along the x-axis. The concentration of solvent is then a rapidly varying function of y, and so we write $c \sim c_0(x, Y, t) + O(\epsilon)$, where $Y = y/\epsilon$, and $\epsilon = O(Pe^{-1/2})$ is a typical value of the finger-width. The pressure satisfies the equation

$$\nabla \cdot \left(\frac{1}{\mu(c)} \nabla p \right) = 0, \tag{2.1}$$

and we therefore seek a solution for the pressure of the form

$$p \sim p_0(x, Y, t) + \epsilon p_1(x, Y, t) + \epsilon^2 p_2(x, Y, t) \ldots, \tag{2.2}$$

from which we find that

$$p_0(x, Y, t) = a(x, t) \int_0^Y \mu(c_0(x, Y', t))\, \mathrm{d}Y' + \hat{p}_0(x, t), \tag{2.3}$$

where a and $\hat{p}_0$ are arbitrary functions of x and t. If we did not take $a = 0$ in the above equation then, since $\mu > 0$, we would find that the pressure grows unboundedly as we shrink ϵ to zero so that $Y \to \infty$. We therefore conclude that the leading-order pressure is independent of Y.

The next-order terms of (2.1) lead us to conclude that

$$p_1(x, Y, t) = b(x, t) \int_0^Y \mu(c_0(x, Y', t)\, \mathrm{d}Y' + \hat{p}_1(x, t), \tag{2.4}$$

where $b(x, t)$ and $\hat{p}_1(x, t)$ are arbitrary functions, and once again to ensure that p_1 remains bounded, and our asymptotic expansion (2.3) remains valid, as $\epsilon \to 0$ we require that $b = 0$. Finally, we look at the $O(1)$ terms of (2.1) from which we find that

$$\frac{\partial p_2}{\partial Y} = -\mu(c_0(x, Y, t)) \frac{\partial}{\partial x} \left(\int_0^Y \frac{1}{\mu(c_0(x, Y', t))} \mathrm{d}Y' \frac{\partial p_0}{\partial x} \right) + \mu(c_0(x, Y, t)) d(x, t), \tag{2.5}$$

where $d(x, t)$ is an arbitrary function of x and t.

As $\epsilon \to 0, Y \to \infty$, we suppose that there is some well-defined local harmonic average of $\mu(c_0(x, Y, t))$, $\mu^*(x, t)$, defined so that for large Y

$$\int_0^Y \frac{1}{\mu(c_0(x, Y', t))} \mathrm{d}Y' \sim \frac{1}{\mu^*(x, t)} Y + O(1). \tag{2.6}$$

Since the viscosity is bounded above zero, the existence of such an average is ensured if, for instance, c_0 is a periodic function of Y, but is also ensured under much weaker assumptions; for example, if c_0 is thought of as a random function then stationarity with respect to Y ensures that a local average may be well defined and, if the randomness is also ergodic, the local average will be the same as the local value of the ensemble average. With the harmonic average of the viscosity thus defined we have that

$$\frac{\partial p_2}{\partial Y} \sim -\mu(c_0)\frac{\partial}{\partial x}\left(\frac{1}{\mu^*}\frac{\partial p_0}{\partial x}\right) Y + O(1), \tag{2.7}$$

and so we find, to ensure that p_2 does not grow unboundedly as $\epsilon \rightarrow 0$, that the leading-order pressure must solve

$$\frac{\partial}{\partial x}\left(\frac{1}{\mu^*}\frac{\partial p_0}{\partial x}\right) = 0, \tag{2.8}$$

and if the applied pressure gradient is such that the mean flux is equal to 1, then the local pressure gradient is simply given by

$$\frac{\partial p_0}{\partial x} = -\mu^*(x, t). \tag{2.9}$$

Note that while the leading-order pressure is independent of Y, the flux of fluid is Y-dependent with $\boldsymbol{u} = (u, v)$ given by

$$u \sim u_0 = -\frac{1}{\mu(c_0(x, Y, t))}\frac{\partial p_0}{\partial x}(x, t) = \frac{\mu^*}{\mu(c_0)}, \tag{2.10}$$

$$v \sim \epsilon v_1 = -\epsilon\frac{1}{\mu(c_0(x, Y, t))}\frac{\partial p_2}{\partial Y}(x, Y, t) = -\epsilon\frac{\partial}{\partial x}\left(\int_0^Y \frac{\mu^*}{\mu(c_0)}\,\mathrm{d}Y'\right) + \epsilon\tilde{v}_1(x, t), \tag{2.11}$$

where $\tilde{v}_1$ in general depends on distant (in Y) boundary conditions; however, $\tilde{v}_1$ may be set to zero if the concentration profile is symmetric about the line $Y = 0$, which might be the case if for instance the concentration is periodic in Y. With the above expressions for the leading-order flux in each direction, we are able to write down the model for the evolution of the concentration of solvent, namely (on suppressing the 0 subscripts from the leading-order concentration)

$$\frac{\partial c}{\partial t} + \frac{\partial}{\partial x}\left(\frac{\mu^*}{\mu(c)}c\right) + \frac{\partial}{\partial Y}\left(\left(-\int_0^Y \frac{\partial}{\partial x}\left(\frac{\mu^*}{\mu(c)}\right)\mathrm{d}Y' + \tilde{v}_1\right)c\right) = \frac{1}{Pe^*}\frac{\partial^2 c}{\partial Y^2}, \tag{2.12}$$

where $Pe^* = \epsilon^2 Pe = O(1)$, since we have assumed that $\epsilon = O(Pe^{-1/2})$.

Equation (2.12) provides our fundamental model for the evolution of the solvent concentration profile in the mixing zone, at least away from the roots and tips of fingers where our large aspect ratio assumption may break down. We shall analyse this model in more detail in § 2.2, but first we shall attempt to use this model to describe the evolution of the averaged concentration of solvent in the style of the Koval model.

2.1. *Averaged model of fingering*

Integrating (2.12) with respect to Y yields

$$\frac{1}{Pe^*}\frac{\partial c}{\partial Y} + \left(\int_0^Y \frac{\partial}{\partial x}\left(\frac{\mu^*}{\mu(c)}\right)\mathrm{d}Y'\right)c - \tilde{v}_1 c = \int_0^Y \left(\frac{\partial c}{\partial t} + \frac{\partial}{\partial x}\left(\frac{\mu^*}{\mu(c)}c\right)\right)\mathrm{d}Y' + e(x, y, t), \tag{2.13}$$

where e is a constant function of integration. For large Y the right-hand side of the above equation is asymptotically equal to

$$\left(\frac{\partial \bar{c}}{\partial t} + \frac{\partial}{\partial x}\left(\mu^*\overline{\frac{c}{\mu(c)}}\right)\right) Y + O(1), \tag{2.14}$$

where $\bar{c}$ is the transverse average of c defined so that

$$\int_0^Y c(x, Y', t)\,\mathrm{d}Y' \sim \bar{c}Y, \tag{2.15}$$

for large Y and $\overline{c/\mu(c)}$ is similarly defined. To ensure that the left-hand side of (2.13) does not grow unboundedly as $Y \to \infty$ we require that

$$\frac{\partial \bar{c}}{\partial t} + \frac{\partial}{\partial x}\left(\mu^{*}\overline{\frac{c}{\mu}}\right) = 0. \tag{2.16}$$

However, (2.16) is not closed since neither μ^{*} nor $\overline{c/\mu(c)}$ is known as a function of $\bar{c}$. One way of closing the model, as noted in Yortsos & Salin (2006), is to assume that diffusion is entirely negligible with a sharp interface between pure oil and pure solvent even on the microscopic scale. The concentration may now only take the values 0 (in the oil) and 1 (in the solvent) and we find that

$$\mu^{*} = \frac{1}{M\bar{c} + 1 - \bar{c}}, \quad \overline{\left(\frac{c}{\mu(c)}\right)} = M\bar{c}, \tag{2.17}$$

which on substitution into (2.16) yields the ‘naïve’ Koval model,

$$\frac{\partial \bar{c}}{\partial t} + \frac{\partial}{\partial x}\left(\frac{M\bar{c}}{M\bar{c} + 1 - c}\right) = 0. \tag{2.18}$$

The naïve Koval model (2.18) is superficially similar to the Koval model (1.5), predicting the same qualitative behaviour; however, it completely fails to predict the correct growth rate of the mixing zone. It is clear that our naïve assumption is not reasonable; diffusion plays an important rôle in the scale of the fingers. While it is possible to derive the Koval model (1.5) by hypothesizing a sharp interface between the oil and a specific mixture of oil and solvent, it is clear from numerical simulations and physical experiments that this can be only thought of as an effective closure condition and does not represent the true physical situation. We have lost information by performing the averaging process that led us from (2.12) to (2.16), and, to be able to more fully understand the relationship between the average concentration and the averages μ^{*} and $\overline{c/\mu(c)}$, and also to explain the growth rate of the mixing zone, we must analyse (2.12) in more detail.

2.2. *Shock formation*

For the remainder of the paper we shall assume that c is a periodic function of Y, although possibly with a period W greater than 1 as shown in figure 1(*b*). We also assume that $Y = 0$ is a line of symmetry such as a symmetric finger tip or root, allowing us to take $\tilde{v}_1 = 0$. The assumption of periodicity is primarily to allow for simpler analysis; however, numerical simulations (see figure 2) appear to exhibit some periodic structure.

Equation (2.12) possesses a few simple solutions, such as solutions independent of x, for which $v_1 = 0$ and so only diffusion acts, and also simple travelling wave solutions independent of Y with $c = c(x - t)$. These travelling wave solutions are unstable to two-dimensional disturbances as shown in Yang *et al.* (2002). Obtaining solutions that represent fingers is somewhat more difficult, and so we have conducted some preliminary numerical investigations. Our numerical simulations indicate that discontinuities in the concentration may form along lines parallel to the Y-axis, suggesting that (2.12) may admit a weak solution with shocks. The shocks form at

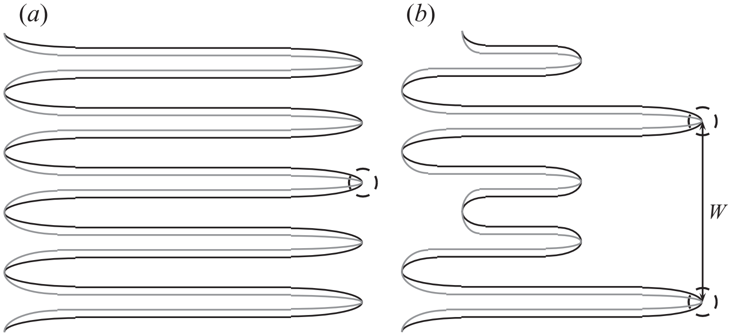

FIGURE 1. Two possible structures of periodic fingering pattern: (*a*) periodic fingers with period 1, (*b*) periodic concentration profile with period $W > 1$.

FIGURE 2. Numerical simulation of miscible viscous fingering (defined in (1.1)–(1.3)) from Booth (2008), with a constant flux of solvent (on left of image) into oil, and $M = 5$, $Pe = 3000$. Numerical simulation uses a high-resolution finite-volume method with flux limiters.

the 'finger tips', the points where the solvent has encroached the furthest into the oil, and the 'finger roots', the point where the oil has remained furthest behind.

An accurate numerical simulation of the model, capable of resolving the speed of the shocks, requires us to solve the problem in conservative form, or equivalently solve a weak formulation of (2.12); however, as we now show, the non-local dependence of the flux on the concentration prevents a standard weak formulation. Since the flow is incompressible we may deduce the existence of a stream function ψ defined by

$$\frac{\partial \psi}{\partial Y} = \frac{\mu^*(x,t)}{\mu(c(x,Y,t))}, \tag{2.19}$$

so that (2.12) becomes

$$\frac{\partial c}{\partial t} + \frac{\partial}{\partial x}\left(\frac{\partial \psi}{\partial Y}c\right) - \frac{\partial}{\partial Y}\left(\frac{\partial \psi}{\partial x}c\right) = \frac{1}{Pe^*}\frac{\partial^2 c}{\partial Y^2}. \tag{2.20}$$

In attempting to derive a weak formulation of the above equation we shall inevitably come across a term of the form

$$\int\int \frac{\partial \phi}{\partial Y}\frac{\partial \psi}{\partial x} c \, \mathrm{d}x \, \mathrm{d}Y, \tag{2.21}$$

where ϕ is our test function. It is not possible to pass the x-derivative of ψ on to the test function ϕ without coincidentally causing an x-derivative of c to appear. We expect c to be discontinuous in x and therefore we also expect ψ to be discontinuous in x; however, it is not possible to express ψ as a function of the local value of c, since ψ depends on the global behaviour of c via μ^*.

It does not therefore appear to be possible to produce a weak formulation of (2.12) for a shock parallel to the Y-axis. An alternative approach to dealing with weak formulations of a problem is to regularize the problem, i.e. re-examine the assumptions that we have made to arrive at (2.12) to find the local behaviour near to the shocks. This approach is considered in the next section.

3. Tip and root modelling

The shocks encountered in the previous section correspond to the tips and roots of fingers. To find the correct behaviour close to shocks in our homogenized model (2.12) we should rescale (1.1)–(1.3) close to tips and roots and then proceed to match with our solution of (2.12) either side of the shock. The rescaling of y by ϵ in § 2 has two effects: firstly, to leading order the pressure may be treated as independent of Y, and secondly, longitudinal diffusion may be neglected. Previous works of Menon & Otto (2005) and Yortsos & Salin (2006) have attempted to explain the observed growth rate of the mixing zone by retaining longitudinal diffusion, using Burgers' model for viscous shocks in gas dynamics as an analogue. Assuming, as we have, that the diffusion in the longitudinal and transverse directions are of the same order of magnitude leads us to conclude that longitudinal diffusion becomes important once the width of the shock is of order ϵ^2. However, the assumption that the pressure is independent of Y breaks down once the width of the shock is of order ϵ, and so we should examine this behaviour first.

If the position of the shock is given by $x = F(t)$, then we consider rescaling near the shock with

$$X = \frac{x - F(t)}{\epsilon} \tag{3.1}$$

and

$$p \sim p_0(t) + \epsilon P(X, Y, t) + \cdots , \tag{3.2}$$

where $p_0(t)$ is the pressure obtained from matching to regions either side of the shock. With these scalings (1.1)–(1.3) becomes

$$\frac{\partial}{\partial X}\left(\frac{1}{\mu(c)}\frac{\partial p}{\partial X}\right) + \frac{\partial}{\partial Y}\left(\frac{1}{\mu(c)}\frac{\partial p}{\partial Y}\right) = 0, \tag{3.3}$$

with the concentration satisfying

$$\begin{aligned}\frac{\partial c}{\partial t} - \frac{U}{\epsilon}\frac{\partial c}{\partial X} - \frac{1}{\epsilon}\frac{\partial}{\partial X}\left(\frac{c}{\mu(c)}\frac{\partial P}{\partial X}\right) - \frac{1}{\epsilon}\frac{\partial}{\partial Y}\left(\frac{c}{\mu(c)}\frac{\partial P}{\partial Y}\right)&\\ + \frac{\partial}{\partial X}(u_1 c) + \frac{\partial}{\partial Y}(v_1 c) = \frac{1}{Pe^*}\left(\frac{\partial^2 c}{\partial X^2} + \frac{\partial^2 c}{\partial Y^2}\right).&\end{aligned} \tag{3.4}$$

The coefficient of $\partial c/\partial t$ is small compared to ϵ^{-1} and so the quasi-steady-state assumption applies with c and P only depending on t through the boundary conditions and through U. After an initial transient where $t = O(\epsilon)$, we have

$$U\frac{\partial c}{\partial X} + \frac{\partial}{\partial X}\left(\frac{c}{\mu(c)}\frac{\partial P}{\partial X}\right) + \frac{\partial}{\partial Y}\left(\frac{c}{\mu(c)}\frac{\partial P}{\partial Y}\right) = 0. \tag{3.5}$$

Equations (3.3) and (3.5) form our model for the tip region and we note that to leading-order diffusion is negligible. This is because the time scale associated with this tip region is very small.

Matching with solutions to (2.12) either side of the shock is necessary to provide the boundary conditions for our tip-scale model. If $c_{\pm}(Y, t)$ are the transverse concentration profiles ahead of and behind the tip/root regions then our boundary conditions are

$$c \to c_{\pm}, \quad \frac{\partial P}{\partial X} \to -\mu^*_{\pm} \quad \text{as} \quad X \to \pm\infty, \tag{3.6}$$

where $\mu^*_{\pm}$ are the harmonic averages of $\mu(c_{\pm})$ (independent of Y). To make further progress we shall restrict ourselves to considering only the leading finger tips, as circled in figure 1, so that $c_+ = 0$ and $\mu^*_+ = 1$. The rate of growth of the leading finger tips governs the rate of growth of the edge of the mixing zone, and so an understanding of the leading finger tips will hopefully provide an explanation for the observed growth rate of the mixing zone. We can easily determine one 'shock condition' at the leading finger tip by requiring that the total flux of fluid into the tip region is equal to the total flux leaving the tip region. By integrating (3.3) we find that

$$U = \frac{\mu^*_-}{W\bar{c}_-}\int_0^W \frac{c_-}{\mu_-}\,\mathrm{d}Y, \tag{3.7}$$

where

$$\bar{c}_- = \frac{1}{W}\int_0^W c_-\,\mathrm{d}Y, \tag{3.8}$$

and W is the period of the fingering pattern, or alternatively the width between leading finger tips expressed as a multiple of the mean finger width as shown in figure 1(*b*). We assume that the leading fingers are symmetric to leading order so that we may take the finger tip to lie on the line of symmetry $Y = 0$. Equations (3.3) and (3.5) together with the boundary conditions (3.6) are invariant under the rescalings

$$X \to \lambda X', \quad Y \to \lambda Y' \quad \text{and} \quad P \to \lambda P',$$

and so we may freely rescale X, Y and P by $W/2$ without altering our problem, and allowing us to solve for a half-finger in $0 < Y < 1$. The period W between leading fingers only appears in the downstream concentration profile where it is a measure of the finger width as a fraction of the separation between fingers.

One particular family of symmetric, weak solutions with discontinuous boundary conditions as $X \to -\infty$ corresponds to Saffman–Taylor fingers. Suppose the downstream concentration profile consists of a particular homogeneous mixture of solvent and oil with solvent concentration c_e, separated from a region of pure oil. The downstream viscosity profile is

$$\mu_-(Y) = \begin{cases} 1/M_e, & 0 < Y < \lambda, \\ 1, & \lambda < Y < 1, \end{cases} \tag{3.9}$$

where $M_e = 1/\mu(c_e)$ and $\lambda \propto 1/W$, and we find from (3.7) that the velocity of the tip is given by

$$U = \frac{M_e}{1 + \lambda(M_e - 1)},$$

as found in Saffman & Taylor (1958). The Saffman–Taylor finger solution is clearly a possible weak solution of (3.3)–(3.5) when periodic fingers are sought. In fact the Saffman–Taylor finger is the only possible solution, when periodic fingers are sought, as we shall now show.

We note that in our tip-scale model (3.3) and (3.5) diffusion does not appear. It is only possible for the oil and solvent to mix in a further inner-inner region, i.e. an inner region of our tip-scale problem located along a sharp jump in the concentration. The rate at which oil mixes with solvent over these inner-inner regions is small, and so we must not only conserve the total mass of fluid and the total mass of solvent, but also the total mass of 'pure oil', i.e. oil that is not mixed with any solvent. The total flux of pure oil upstream must therefore be equal to the total flux of pure oil downstream, ensuring that there must be a finite-width region of pure oil downstream of the finger tip. If this region is given by $\lambda < Y < 1$, then we find from equating the flux of pure oil upstream and downstream of the finger tip that

$$(1 - \lambda)(\mu_-^* - U) = 1 - U, \tag{3.10}$$

where as before

$$\frac{1}{\mu_-^*} = \int_0^1 \frac{1}{\mu(c_-(Y))}\,\mathrm{d}Y.$$

Using (3.7) to find U, (3.10) becomes

$$1 - \lambda + \frac{\lambda}{\bar{c}_-}\int_0^1 \frac{c_-(Y)}{\mu(c_-(Y))}\,\mathrm{d}Y = \frac{1}{\mu_-^*}.$$

We can write

$$\begin{aligned}\int_0^1 \frac{1}{\mu(c_-(Y))}\,\mathrm{d}Y &= \int_0^\lambda \frac{1}{\mu(c_-(Y))}\,\mathrm{d}Y + \int_\lambda^1 \mathrm{d}Y \\ &= 1 - \lambda + \int_0^\lambda \frac{1}{\mu(c_-(Y))}\,\mathrm{d}Y,\end{aligned}$$

and so we obtain the condition that

$$\frac{\lambda}{\bar{c}_-}\int_0^1 \frac{c_-(Y)}{\mu(c_-(Y))}\,\mathrm{d}Y = \int_0^\lambda \frac{1}{\mu(c_-(Y))}\,\mathrm{d}Y,$$

or, since $c_-(Y) = 0$ in $\lambda < Y < 1$,

$$\int_0^\lambda \frac{c_-(Y)}{\mu(c_-(Y))}\,\mathrm{d}Y = \frac{1}{\lambda}\int_0^\lambda c_-(Y)\,\mathrm{d}Y \int_0^\lambda \frac{1}{\mu(c_-(Y))}\,\mathrm{d}Y. \tag{3.11}$$

However, since μ is a monotonic decreasing function of c we require that

$$\frac{1}{\lambda}\int_0^\lambda \frac{c_-(Y)}{\mu(c_-(Y))}\,\mathrm{d}Y \geqslant \frac{1}{\lambda^2}\int_0^\lambda c_-(Y)\,\mathrm{d}Y \int_0^\lambda \frac{1}{\mu(c_-(Y))}\,\mathrm{d}Y,$$

with equality if and only if $c_-(Y)$ is constant in $0 < Y < \lambda$. Since (3.11) implies that equality holds we see that $c_-(Y)$ must be constant in $0 < Y < \lambda$, and the only permissible downstream concentration profile corresponds to that of the

Saffman–Taylor finger with a region of oil separated from a region with a constant concentration of solvent. This result implies that the only possible tip-scale solution corresponds to a Saffman–Taylor finger.

Equations (3.3) and (3.5) admit Saffman–Taylor finger solutions with arbitrary width λ, and therefore allow a wide range of possible speeds for the growth of the mixing zone. The growth rate of the leading edge of the mixing zone depends on both the separation of the leading finger tips and also the concentration of solvent in the leading finger tips. We have not excluded the possibility that the leading finger tips consist of a homogeneous mixture of solvent and oil, rather than pure solvent. It has proved possible to explain the selection of the $\lambda = 1/2$ Saffman–Taylor finger by the introduction of both surface tension (Combescot *et al.* 1986; Chapman 1999) and kinetic undercooling (Chapman & King 2003) as regularizations of the Muskat problem, and it has been suggested in Chapman & King (2003) that the $\lambda = 1/2$ solution might be expected to be chosen for most possible regularizations. If the $\lambda = 1/2$ solution is taken for this problem, we do indeed find that the growth rate of leading fingers is lower than that predicted by naïve modelling, yet the growth rate still does not match the data of Blackwell *et al.* (1959). For mobility ratios close to 1, the $\lambda = 1/2$ solution overpredicts the growth, at least if the finger contains pure solvent at the tip. For large mobility ratios the $\lambda = 1/2$ solution severely underpredicts the growth of the finger, regardless of the value of the assumed concentration of solvent in the finger tip.

It is worth noting that the introduction of diffusion does not appear to allow a similar analysis to that in Chapman & King (2003); in particular, it is not possible to treat the displacing fluid as a rigid body, and so the finger-width may be dependent on the mobility ratio. It is possible that the introduction of diffusion does not lead to the usual $\lambda = 1/2$ solution, and this may then explain the observed growth rate.

4. Conclusions

The Koval model appears to be an accurate representation of the averaged concentration profile in miscible viscous fingering when $Pe \gg 1$. In this regime many long thin fingers are formed, and the large aspect ratio of these fingers ensures that the pressure is largely constant transverse to the direction of finger growth. Simple averaging across the fingers leads to an underdetermined problem, and therefore further analysis of the model prior to averaging is required. This analysis in turn requires us to understand the behaviour near the roots and tips of fingers; this behaviour governs the growth of the fingers and hence the growth of the mixing zone.

At the leading finger tips we have shown that the only permissible solutions correspond to Saffman–Taylor fingers, implying the persistence of a reasonably sharp jump between solvent and oil in these tip regions. In the contour plots of many high-resolution numerical simulations (see Zimmerman & Homsy 1991; Rogerson & Meiburg 1993) a sharp jump between solvent and oil can be seen near the finger tips for large Pe. The shape selection of Saffman–Taylor fingers has been a challenging problem in immiscible flow with small surface tension playing a crucial role. For our problem, further analysis is required of the effect that small diffusion has near the almost sharp interface predicted at miscible finger tips. The introduction of even very small diffusion seemingly requires us to abandon a free boundary problem formulation of the model, and it is not then clear how arguments for shape selection by other regularization mechanisms may be adapted to this situation.

Our modelling differs from some previous works (Menon & Otto 2005; Yortsos & Salin 2006) in that our regularization of shocks in (2.12) is provided by a two-dimensional model of the finger tips, rather than by the retention of longitudinal diffusion. The retention of longitudinal diffusion is appropriate when the ratio between longitudinal and transverse diffusion is large so that the Péclet numbers for longitudinal and transverse diffusion ($Pe_\parallel$ and $Pe_\perp$, respectively) satisfy $Pe_\parallel \leqslant O(1)$ and $Pe_\perp \gg 1$. This is a conceivable physical regime for flow in a porous medium, but numerical simulations (Yang *et al.* 2002; Booth 2008) show that the Koval model maintains good agreement with solutions to (1.1)–(1.3) when in each direction the diffusion is of the same order of magnitude.

One failing of our model is the assumption that the mean finger width does not vary over time. As noted in Menon & Otto (2005) the mean finger width should grow proportional to the square root of time; however, the mechanism by which this mean growth occurs does not appear to be simple, apparently being caused by slow transverse diffusion followed by rapid convective coalescence of fingers as noted in Zimmerman & Homsy (1991). As it stands our model is not capable of predicting the long-time convective evolution of the mixing zone. The mean value of Pe^* is then proportional to $1/t$, which allows for a convective similarity variable x/t. This can be explained phenomenologically by the gradual growth of the mean finger width at a rate proportional to $t^{1/2}$. The growth of the mixing zone is still controlled by a solution of the finger-tip problem.

This research was supported by a joint CASE studentship between EPSRC and Schlumberger. The author would like to thank his supervisors Dr C. L. Farmer and Professor J. R. Ockendon.

REFERENCES

Blackwell, R. J., Rayne, J. R. & Terry, W. M. 1959 Factors influencing the efficiency of miscible displacement. *Trans. AIME* **216**, 1–8.

Booth, R. J. S. 2008 Miscible flow through porous media. PhD thesis, Oxford University, Oxford, UK.

Chapman, S. J. 1999 On the rôle of Stokes lines in the selection of Saffman–Taylor fingers with small surface tension. *Eur. J. Appl. Math.* **10**, 513–534.

Chapman, S. J. & King, J. R. 2003 The selection of Saffman–Taylor fingers by kinetic undercooling. *J. Engng Math.* **46**, 1–32.

Chen, C.-Y. & Meiburg, E. 2000 High-accuracy implicit finite-difference simulations of homogeneous and heterogeneous miscible-porous-medium flows. *SPE J.* **5**, 129–137.

Christie, M. A., Muggeridge, A. H. & Barley, J. J. 1993 3D simulation of viscous fingering and WAG schemes. *SPE J.* **8**, 19–26.

Combescot, R., Hakim, V., Dombre, T., Pomeau, Y. & Pumir, A. 1986 Shape selection of Saffman–Taylor fingers. *Phys. Rev. Lett.* **56**, 2036–2039.

Fayers, F. J. 1988 An approximate model with physically interpretable parameters for representing viscous fingering. *SPE Reservoir Engng* **285**, 551–558.

Fayers, F. J., Blunt, M. J. & Christie, M. A. 1992 Comparisons of empirical viscous-fingering models and their calibration for heterogeneous problems. *SPE Reservoir Engng*, pp. 195–203.

Hickernell, F. J. & Yortsos, Y. C. 1986 Linear stability of miscible displacement processes in porous media in the absence of dispersion. *Stud. Appl. Math.* **74**, 93–115.

Homsy, G. M. 1987 Viscous fingering in porous media. *Annu. Rev. Fluid Mech.* **19**, 271–311.

Koval, E. J. 1963 A method for predicting the performance of unstable miscible displacement in heterogenous media. *SPE J.* **450**, 145–154.

Manickam, O. & Homsy, G. M. 1995 Fingering instabilities in vertical miscible displacement flows in porous media. *J. Fluid Mech.* **288**, 75–102.

Menon, G. & Otto, F. 2005 Dynamic scaling in miscible viscous fingering. *Commun. Math. Phys.* **257**, 303–317.

Mikelić, A. 1993 Regularity and uniqueness results for two-phase miscible flows in porous media. *Intl. Ser. Numer. Math.* **114**, 139–154.

Peaceman, D. W. & Rachford, H. H. 1962 Numerical calculation of multidimensional miscible displacement. *SPE J.* **2**, 327–339.

Riaz, A. & Meiburg, E. 2003 Three-dimensional miscible displacement simulations in homogeneous porous media with gravity override. *J. Fluid Mech.* **494**, 95–117.

Riaz, A., Pankiewitz, C. & Meiburg, E. 2004 Linear stability of radial displacements in porous media: influence of velocity-induced dispersion and concentration-dependent diffusion. *Phys. Fluids* **16**, 3592–3598.

Rogerson, A. & Meiburg, E. 1993 Numerical simulation of miscible displacement processes in porous medium flows under gravity. *Phys. Fluids* A **5**, 2644–2660.

Ruith, M. & Meiburg, E. 2000 Miscible rectilinear displacements with gravity override. Part 1. Homogeneous porous medium. *J. Fluid Mech.* **420**, 225–257.

Saffman, P. G. & Taylor, G. I. 1958 The penetration of a fluid into a porous medium or Hele-Shaw cell containing a more viscous fluid. *Proc. R. Soc.* A **245**, 312–329.

Siegel, M., Caflisch, R. E. & Howison, S. D. 2004 Global existence, singular solutions, and ill-posedness for the Muskat problem. *Commun. Pure Appl. Math.* **LVII**, 1374–1411.

Tan, C. T. & Homsy, G. M. 1986 Stability of miscible displacements in porous media – rectilinear flow. *Phys. Fluids* **29**, 3549–3556.

Tan, C. T. & Homsy, G. M. 1988 Simulation of nonlinear viscous fingering in miscible displacement. *Phys. Fluids* **31**, 1330–1338.

Tchelepi, H. A. & Orr, F. M., Jr. 1994 Interaction of viscous fingering, permeability heterogeneity, and gravity segregation in three dimensions. *SPE Reservoir Engng* **9**, 266–271.

Tchelepi, H. A., Orr, F. M., Jr., Rakotomalala, N., Salin, D. & Wouméni, R. 1993 Dispersion, permeability heterogeneity, and viscous fingering: acoustic experimental observations and particle-tracking simulations. *Phys. Fluids* A **5**, 1558–1574.

Todd, M. R. & Longstaff, W. J. 1972 The development, testing and application of a numerical simulator for predicting miscible flood performance. *J. Pet. Tech.* **253**, 874–882.

Wooding, R. A. 1969 Growth of fingers at an unstable diffusing interface in a porous medium or Hele-Shaw cell. *J. Fluid Mech.* **39**, 477–495.

Yang, Z. M., Yortsos, Y. C. & Salin, D. 2002 Asymptotic regimes in unstable miscible displacements in random porous media. *Adv. Water Resour.* **25**, 885–898.

Yortsos, Y. C. & Salin, D. 2006 On the selection principle for viscous fingering in porous media. *J. Fluid Mech.* **557**, 225–236.

Zimmerman, W. B. & Homsy, G. M. 1991 Nonlinear viscous fingering in miscible displacement with anisotropic dispersion. *Phys. Fluids* A **3**, 1859–1872.

Zimmerman, W. B. & Homsy, G. M. 1992 Viscous fingering in miscible displacements: unification of effects of viscosity contrast, anisotropic dispersion, and velocity dependence of dispersion on nonlinear finger propagation. *Phys. Fluids* A **4**, 2348–2359.